A Thermodynamic Prediction of Tie Chain Length Distribution in Drawn Semicrystalline Polymers

RAKESH POPLI* *and* DAVID ROYLANCE

Department of Materials Science and Engineering
Massachusetts Institute of Technology
Cambridge, Massachusetts 02139

The mechanism underlying fracture of many oriented semicrystalline polymers is hypothesized to be a thermally activated, stress-aided rate process in which the tie chains connecting crystalline units suffer thermomechanical dissociation. Some previous numerical models based on this concept have assumed a Gaussian distribution of tie chain contour lengths which are ruptured progressively by successively higher specimen strains, and have used electron spin resonance (ESR) spectroscopy to obtain the numerical parameters of the distribution. The distribution of tie chain lengths in the intercrystalline region is calculated theoretically in this paper, based on minimization of free energy. Our results, although in basic agreement with earlier models, suggest a reinterpretation of some of the ESR findings with regard to molecular fracture processes.

INTRODUCTION

Many highly drawn semicrystalline polymers consist of alternating crystalline and amorphous regions making up a fibrillar microstructure. The amorphous regions consist in turn of three types of molecular chain segments: loops or folds at the interface between crystalline and amorphous blocks, chains which end within the amorphous region ("cilia"), and tie chains bridging the amorphous region so as to connect adjacent crystalline blocks. The tie chains are the principal load-bearing elements within the fibrillar structure, and this paper seeks to predict their length distribution. This will be done by considering the free energies of tie molecules of various lengths present in the intercrystalline space. The model will be developed using the microstructure of drawn polyamide fibers as a guide, and the numerical constants will be those which apply to that system, but the results should be applicable with some modification to other drawn semicrystalline polymers as well.

One of the central problems in developing atomistic models for the fracture of solids is that of specifying just how the applied stresses are distributed over the specimen's internal microstructure. For some polymers, it has been possible to provide an experimental measure of this stress distribution by using analytical chemical methods to monitor the mechanochemical changes which accompany fracture in these materials. Electron spin resonance spectroscopy (ESR) has been particularly valuable in this regard, since it is able to monitor the free radicals which are produced by homolytic scission of the polymer molecule.

ESR has been used to monitor stress-induced bond rupture in drawn polyamide fibers, and *Fig. 1* shows a typical histogram giving the extent of bond scission at various specimen strains (1, 2). Kausch and DeVries (3) interpreted this histogram as representing the distribution of contour lengths of the tie chains connecting the crystalline segments of the microfibrillar structure, and based their calculation of the internal stress distribution on this assumption. However, this interpretation is controversial, as other microstructural distributions can also be hypothesized as leading to the observed ESR histogram. The theoretical tie chain length model to be developed in this paper will be used to argue that the ESR histogram does not in fact reflect the entire tie chain length distribution, and that in most amorphous regions only the shortest 5 percent of the tie chains are broken during the fracture process.

THEORETICAL MODEL

We will obtain a theoretical estimate of the tie chain length distribution by seeking a minimum in the expression for the chain's free energy. Our treatment assumes a basic model of the semicrystalline polymer consisting of two crystalline blocks and an amorphous region separating them (*Fig. 2*). Of course, this represents only a small building

* Present address: S. C. Johnson & Sons, Racine, WI 53403.

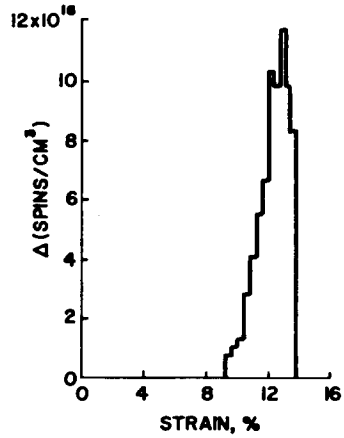

Fig. 1. Histogram of free radical concentration obtained in step-strain loading of polyamide fibers at room temperature (from Ref. 2).

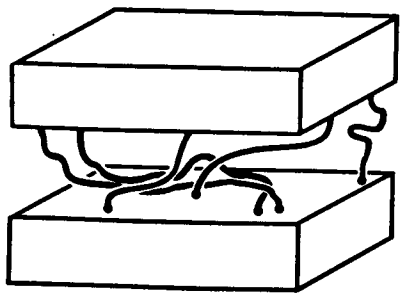

Fig. 2. Schematics of typical crystalline and amorphous regions in drawn semicrystalline polymers.

block of the complex morphology present in drawn polymer fibers. The block shown in *Fig. 2* is repeated thousands of times along the microfibrillar structure, and many microfibrils in turn are stacked alongside one another to make up the small fibrils which can be observed microscopically or sometimes with the unaided eye. However, the tie-chain and block model has been used by many previous researchers as containing the essential physics of the fiber's mechanical response, in that the tie chain length distribution is argued to be the essential feature governing strength and stiffness. This is the assertion which will be explored in this paper.

In the morphological model of *Fig. 2*, the tie molecule is viewed as a chain which traverses a cubic lattice between two crystallite surfaces. The free energy of the element consists of the energy contribution from the crystalline blocks, the amorphous region, and the interfacial region between them. This free energy F can be written as:

$$F = [M - \sum \nu_N N]F_c + \sum \nu_N F_L(N) + kT \sum ln\,(\nu_N/\nu) + 2\nu\sigma + \sigma' \quad (1)$$

where the summations are over all tie chains ν_N and the other symbols are defined as:

M = Total number of model units present in the element of *Fig. 2*.

F_c = Energy of a model unit length in the crystalline block.

$F_L(N)$ = Energy of a tie chain of N units and length L.

ν_N = Number of tie chains of N units.

ν = Total number of tie chains present in the element.

σ = Surface energy per tie chain.

σ' = Total surface energy of chain loops.

The tie chain distribution function $G(N)$ is obtained by minimizing the free energy F subject to the condition that $\nu = \sum \nu_N$ = constant. Using *Eq. 1* and setting $\delta F = 0$ gives the distribution function:

$$G(N) = (\nu_N/\nu) = \exp[-\Delta F_L(N)/kT]/\{\sum \exp[-\Delta F_L(N)/kT]\} \quad (2)$$

where $\Delta F_L(N) = F_L(N) - NF_c$. The free energy $\Delta F_L(N)$ consists of an enthalpy and an entropy term, $\Delta F_L = \Delta H_L - T\Delta S_L$, where T is the equilibrium thermodynamic temperature at which the fibrillar structure is formed. This is taken as the drawing temperature, typically some value less than the crystalline melting temperature.

The enthalpy term $\Delta H_L(N)$ is the enthalpy of melting for N crystalline units, plus a term due to chains in the interfacial zone. Chain segments in the interfacial zone experience additional constraint due to the proximity of their neighbors, and the enthalpy of such segments is different than that of crystalline or amorphous segments:

$$\Delta H_L(N) = N\Delta H^\circ + \gamma^\circ \quad (3)$$

Here ΔH° is the melt enthalpy of a unit length of crystalline chain and γ° is the interfacial constraint energy. We assume that all the tie chain constraints are confined to a small interfacial zone as shown in *Fig. 3*, and that the interfacial constraint energy for each tie chain is independent of its length.

The entropy $S_L(N)$ of a tie chain of length L and N units differs from that of a chain of the same length in the amorphous polymer melt, since the ends of the tie chain are fixed at the crystal and the tie chains are confined to the volume between the two crystalline blocks. We write:

$$S_L(N, r) = S'(N) + k\ ln[Z^\circ(N, r)] \quad (4)$$

where S' is the entropy contribution arising from inner vibrations of the chain, and the second term accounts for the number of tie chain configurations $Z^\circ(N, r)$ in the amorphous region.

Zachman and Peterlin (4) give the configuration function $Z^\circ(N, r)$ of a chain fixed at two ends as:

$$Z^\circ(N, r) = W(N + 1, r)\ Z'(N + 1)a^3 \quad (5)$$

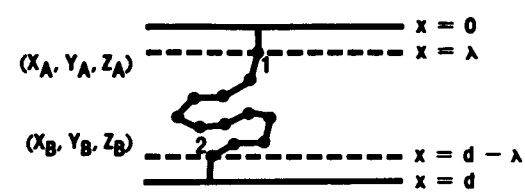

Fig. 3. Schematic drawing of a tie molecule in an amorphous region. Interfacial zone boundary is indicated by dashed lines at $x = \lambda$ and $x = d-\lambda$. Solid lines at $x = 0$ and $x = d$ represent crystalline faces.

where $W(N+1, r)a^3$ is the probability that the end of the model chain is enclosed in a volume a^3 at a distance r from the other chain end. $Z'(N+1)$ is the number of configurations of a chain of $N+1$ units with both ends free (as in the melt); for a cubic lattice it is equal to 6^{N+1} (5).

For calculation purposes, the interfacial zone has been chosen to be of width 2a (4.92A°) and the chain has only one possible configuration in this region. Therefore the shortened chain of $N-2$ units connecting points 1 and 2 in the amorphous region shown in *Fig. 3* has the same number of configurations as the entire tie chain of $N+2$ units:

$$Z^{\circ}(N+2, r) = Z'(N-1)\, P(N, r)$$

The probability $P(N, r)$ of a given configuration with end-to-end distance r for a chain of $N-2$ units in the volume limited by the crystal faces is the probability of chain configuration in infinite space minus the probability for those configurations which partly touch, or cross either or both of the crystal faces (4, 6, 7), and is given as

$$P(N, r) = a^3 \sum_{m=-\infty}^{\infty} [W(x_1 - x_2 - 2md, y, z) - W(x_1 + x_2 - 2md, y, z)] \quad (6)$$

where (x_1, y_1, z_1) and (x_2, y_2, e_2) are the coordinates of the chain ends, $y = y_1 - y_2$, $z = z_1 - z_2$, d is the width of the amorphous region, and W is the statistical distribution function. The computation of $P(N, r)$ using a Gaussian distribution for W is given in an appendix to this paper. The entropy term is then:

$$\Delta S_L(N+2) = (N+2)\Delta S^{\circ} + k\, ln\, P(N, r) - 3k\, ln\, 6 \quad (7)$$

Using *Eqs 3* and *7*, the free energy $\Delta F_L(N+2)$ of a tie chain of $N+2$ units is

$$\Delta F_L(N+2) = (N+2)\Delta H^{\circ} - T[(N+2)\Delta S^{\circ} + k\, ln\, P(N, r) - 3k\, ln\, 6] \quad (8)$$

Factoring and using the thermodynamic relation $\Delta S^{\circ} = \Delta H^{\circ}/T_m$ (T_m being the equilibrium crystalline melting temperature), this becomes:

$$\Delta F_L(N+2) = (N+2)\Delta H^{\circ}\Delta T - kT\{ln\, P(N, r) - 3\, ln\, 6\} \quad (9)$$

where $\Delta T = (T_m - T)/T_m$.

Now knowing $\Delta F_L(N)$ and using the values of various parameters given in *Table 1*, *Eq 2* gives the tie chain length distribution $G(N)$. The model unit length 'a' was taken as 2.46A°, based on a comparison of the entropies of the model and real chains.

The tie chain length distribution function $G(N)$ of the crystalline structure of *Fig. 2* is computed as follows: Each of the crystalline/amorphous boundary crossections is divided into 100 elements of approximately equal area, and coordinates r, θ are assigned. G_{ij} is calculated from *Eq 2* for a chain of end-to-end distance r_{ij} between the ith element on face 1 and the jth element on face 2 of the crystallites. The G_{ij} values for all i and j are averaged to obtain the tie chain length distribution function $G(N)$. A plot of $G(L)$ *vs.* L is shown in *Fig. 4* for various temperatures T and distances L°, where L° is the minimum tie chain length and is equal to the thickness of the amorphous gap between two crystalline lamellar blocks.

DISCUSSION OF THEORETICAL APPROACH

Our treatment assumes equilibrium, although in real polymers the molecular configurations in the amorphous regions are probably dominated more by kinetic than equilibrium considerations. We hope such an equilibrium model is reasonable, even if only to a first approximation.

Also, in the above calculation no consideration for the effects of drawing on the distributions of tie chain lengths has been taken into account. These changes will be small for fibers obtained by cold drawing a semicrystalline starting material, where lamellae are fragmented and a partial melting-recrystallization occurs (8), establishing a new microfibrillar structure. Since recrystallization occurs under stress, the concentration of taut tie molecules will be expected to be somewhat higher than predicted on the basis of the model presented above.

Itoyama (9) obtained a distribution of tie chain lengths and the average tie chain length using a partition-function calculation for stacked lamellae of alternating crystalline and amorphous regions. The generating functions for loops, tie chains, and cilia were calculated using probabilities for random walk on a body-centered cubic lattice in the presence of two parallel walls, and the length distributions of the various chain types were then obtained

Table 1. Numerical Parameters Used in Model

Item	Value	Source
Crystallinity	50.0%	X-ray diffraction "Hdbk. Polym. Sci."
Melting temperature (T_m)	496K	
Processing temperature (T)	428K	Park (18)
Crystalline block length	60A	Park (18)
Amorphous block length (d)	30A	Park (18)
Enthalpy of fusion (ΔH°)	22.7 kJ/mole	van Krevelen (19)
Fibril diameter	80A	Prevorsek (20)

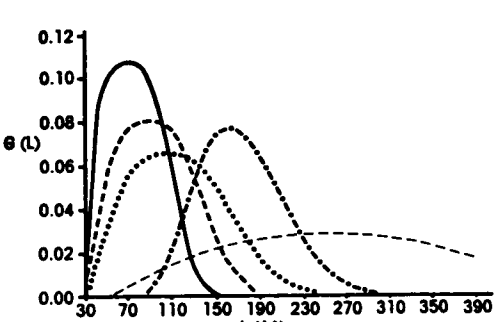

Fig. 4. Density distribution function G(L) vs. tie chain length. Curve A (——): d = 30A, T = 350 K. Curve B (– – –): d = 30A, T = 400K. Curve C (●●●): d = 30A, T = 428K. Curve D (— —): d = 30A, T = 486K. Curve E (–●–●–): d = 60A, T = 428K.

from the partition functions. The Itoyama calculation constrains only the total number of segments present in the system, whereas the thermodynamic equilibrium calculation described in this paper additionally requires minimization of free energy. This results in considerable simplicity in mathematical evaluation of the density distribution for the tie chain lengths.

We have replotted Itoyama's results for the tie chain length distibution in *Fig. 5*. *Figures 4* and 5 exhibit the same general features: Firstly, with increasing value of the crystallization temperature T in the calculation, the maxima in the distribution of tie chain lengths shifts to larger values and the distribution also becomes broader. This is shown by plots A, B, C, and D in *Fig. 4* and plots B and C in *Fig. 5*. Secondly, if the width of the amorphous gap (the length 'd') is increased for a constant temperature T, the tie chain distribution maxima again shifts to greater lengths shown by plots C and E in *Fig. 4* and plots A and B in *Fig. 5*. Therefore, although the detailed descriptions for obtaining the tie chain length distribution for the two models are different, the general features predicted are the same.

CONSEQUENCES FOR FRACTURE BEHAVIOR

Fracture is an extremely complicated phenomenon, undoubtedly involving the rupture or motion of several distributions of load-bearing structural elements of widely different sizes. But in the case of drawn polyamide fibers the evidence seems to support a two-part concept in which the tie chains are distributed in length as described in this paper. The amorphous regions containing these tie chains are also "distributed" in that they respond to the applied specimen strain to varying degrees. However, it appears that this latter distribution can be described simply as a bimodal one in which most amorphous regions are "moderately" strained during fracture so as to experience scission of only the shorter members of their tie chain populations. A much smaller number of amorphous regions—perhaps those near microfibril ends or other defect sites—are so highly strained that all their tie chains are ruptured during the fracture process. Formation of submicrovoids observed using small-angle X-ray scattering (10) supports the existence of these critically situated amorphous regions.

Kausch (11) notes specifically that the buildup of large elastic strains in fibers or films—as evidenced by chain scission (12) and the appearance of distorted infrared spectroscopic bands (13–15)—occurs simultaneously with submicrocrack formation which apparently leads to relief of local stress through retraction of microfibril ends. Kausch feels these processes must therefore occur independently of each other. Such an independence of stress-induced effects can only result from a distribution of stress criticality among various amorphous regions.

A plot of cumulative tie chain distribution function $Q(L)$ *vs.* L/L° is shown in *Fig. 6*, and we can use this function to estimate the fraction of tie chains which will be broken when the specimen is strained to failure. The macroscopic strain to break for polyamide fibers is 15 percent, and at fracture the strain in the amorphous region will be nearly double this. (The crystallinity in the polyamide fiber is 50 percent, and most of the strain occurs in the amorphous phase.) Therefore assuming that all the tie chains of length L/L° less than 1.3 will be ruptured during specimen fracture, a concentration of approximately 5 percent for these "taut" tie chains of the total tie chain population is predicted.

This taut tie chain concentration of approximately 5 percent of the total tie chains present in polyamide fibers as estimated above is in reasonable agreement with other observations: Peterlin (16) indicated a taut tie molecular fraction of 1 to 4

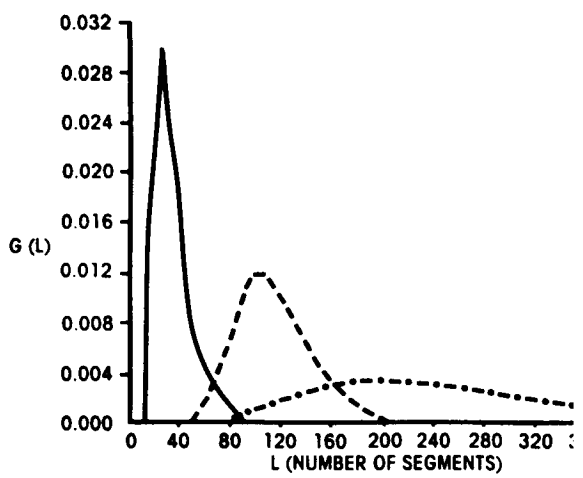

Fig. 5. Density distribution function G(L) vs. tie chain length calculated by Itoyama (Ref. 9) Curve A: (——) d = 16 units, T = 373K. Curve B (– – –): d = 40 units, T = 373K. Curve C (–●–●–): d = 40 units, T = 393K.

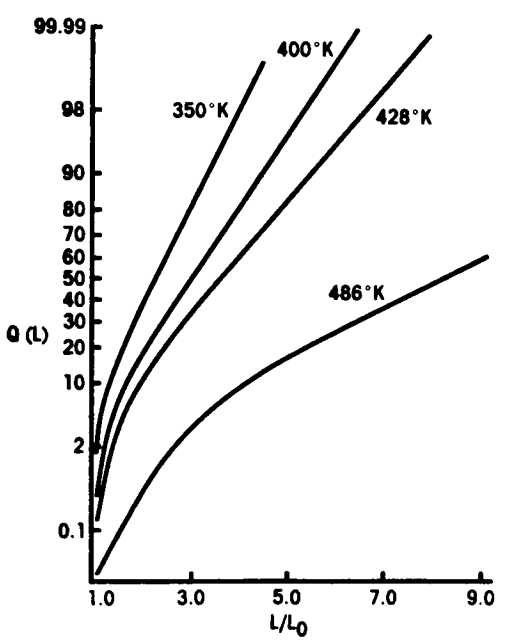

Fig. 6. Cumulative percentage of tie chains Q(L) vs. L/L_o at various temperatures.

percent based on models of the elastic modulus, and Nagou (17) has obtained from results on highly drawn polypropylene a concentration of taut tie molecules of 2 percent in a total concentration for the amorphous phase of 25 percent.

The predicted distribution of chain lengths calculated above shows a variation of the L/L° ratio from one to between five and ten, depending upon the drawing temperature T (see *Fig. 4*). In comparison, Kausch (1) and DeVries (2, 3) calculated an L/L° ratio varying from 1.0 to 1.2, assuming the ESR histogram to reflect the tie chain length distribution. Thus a large difference exists in the widths of tie chain length distribution obtained from the calculation in this manuscript and the models of Kausch and DeVries.

The initial portion of the chain length distribution from the calculation derived here and the Kausch-DeVries results are compared in *Fig. 7*. The ordinate (cumulative number of tie chains) has been scaled so that the total cumulative number of tie chains are the same (taken as unity here) for the theoretical model and the Kausch model at (L/L°) of 1.18. This value of (L/L°) in Kausch's model corresponds to the macroscopic fracture of the specimen.

These results suggest that the Kausch-DeVries distribution does not represent the distribution of all the tie chains, but may reflect only a contribution from the short taut tie chains. The observed free radicals result from rupture of taut tie molecules ($L/L^\circ < 1.3$) which have been stretched to their breaking strain in the amorphous regions throughout the specimen, as well as the rupture of essentially all tie molecules in some more critically situated amorphous regions which may then open up as microcracks. Only approximately 5 percent of the tie chains have been damaged during straining of the specimen to failure, and the fragments left by that failure can be expected to have essentially the same stress-strain curve and failure point as the virgin specimen.

ACKNOWLEDGMENTS

The authors gratefully acknowledge the support of this work by the US Army Research Office under Contract DAAG29-76-0044, and the many helpful suggestions made by Dr. Jeanne Courter.

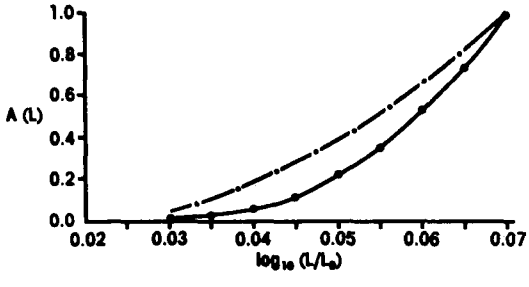

Fig. 7. Cumulative fraction of tie chains vs. log (L/L_o) between $L/L_o = 1.06$ and 1.18. (–●–●–) is this calculation; (–●–●–) is from Kausch (Ref. 1). Graphs scaled to make cumulative fraction equal to one at $L/L_o = 1.18$.

APPENDIX I—CALCULATION FOR P(N, R)[a]

$$P(N, r) = \sum_{m=-z}^{z} [W(N-1, r(m)) - W(N-1, R(m))] \cdot a^3$$

Define $P'(N, r) = P(N, r)/a^3$

$$= \sum_{-z}^{z} [W(N-1, (x_A - 2md, y, z)) - W(N-1, (x_A + \lambda - 2md, y, z))]$$

Using gaussian statistics for tie chain lengths

$$W(r) = [3/2\pi\langle r^2\rangle_o]^{3/2} \cdot \exp(-3r^2/2\langle r^2\rangle_o)$$

where $r^2 = x^2 + y^2 + z^2$

Let $RSQR = y^2 + z^2$

$$P'(N, r) = (3/2\pi\langle r^2\rangle_o)^{3/2} \cdot \exp(-3(RSQR + \lambda^2)/2\langle r^2\rangle_o) \cdot \sum_{m=-z}^{z} \exp(-3(x_A - 2md)^2/2\langle r^2\rangle_o) \cdot 2\sinh(3\lambda(x_A - 2md)/\langle r^2\rangle_o)$$

$$= 2\,C \sum_{m=-z}^{z} \exp(-3(x_A - 2md)^2/2\langle r^2\rangle_o) \cdot \sinh(3\lambda(x_A - 2md)/\langle r^2\rangle_o)$$

where $C = (3/2\pi\langle r^2\rangle_o)^{3/2} \cdot \exp(-3(RSQR + \lambda^2)/2\langle r^2\rangle_o)$

Consider the summation

$$\sum_{m=-z}^{z} = \sum_{m=-z}^{-1} + P'(N, r)/_{m=o} + \sum_{m=1}^{z}$$

Changing variable in one of the summation above we obtain

$$P'(N, r) = 2\,C \exp(-3x_A^2/2\langle r^2\rangle_o) \cdot \sinh(3\lambda x_A/\langle r^2\rangle_o) + \sum_{m=1}^{z} [\exp(-3(x_A - 2md)^2/2\langle r^2\rangle_o) \cdot \sinh(3\lambda(x_A - 2md)\langle r^2\rangle_o) - \exp(-3(x_A + 2md)^2/2\langle r^2\rangle_o) \cdot \sinh(3\lambda(x_A + 2md)/\langle r^2\rangle_o)]$$

Higher order terms in the summation decrease rapidly, therefore keeping only the zeroth and first order terms in the expansion above, using $\lambda = 2a$ and for gaussian statistics $\langle r^2\rangle_o = (N-1)a^2$, we get

$$\log_e P(N, r) = -0.4158 - 1.5 \log_e(N-1) - 1.5(RSQR + 4a^2)/(N-1)a^2 + \log_e[\exp(-3(d-2a)^2/2(N-1)a^2) \cdot \sinh(6(d-2a)/(N-1)a) - \exp(-3(d+2a)^2/2(N-1)a^2) \cdot \sinh(6(d+2a)/(N-1)a)]$$

a) For detailed calculation see reference 21.

REFERENCES

1. H. H. Kausch and J. Becht, *Rheologica Acta*, **9,** 137, (1970).
2. B. A. Lloyd, K. L. DeVries, and M. L. Williams, *J. Polym. Sci., A-2,* **10,** 1415, (1972).
3. H. H. Kausch and K. L. DeVries, *Int. J. Fracture,* **11,** 727, (1975).
4. H. G. Zachman and A. Peterlin, *J. Macromol. Sci.-Phys.*, **B3,** 495, (1969).
5. P. J. Flory, "Principles of Polymer Chemistry," Cornell Univ. Press, (1953).
6. S. Chandrasekhar, *Rev. Mod. Phys.*, **15,** 1, (1943).
7. R. J. Gaylord and D. J. Lohse, *J. Chem. Phys.*, **65,** 2779, (1976).
8. G. D. Wignall and W. Wu, *Polym. Comm.*, **24,** 354, (1983).
9. K. Itoyama, *J. Polym. Sci.-Phys.*, **19,** 1873, (1981).
10. S. N. Zhurkov, V. A. Zakrevskii, V. E. Korsukov, and V. S. Kuksenko, *Soviet Phys.-Solid State,* **13,** 1680, (1972).
11. H. H. Kausch, "Polymer Fracture," Springer-Verlag, (1978).
12. D. Roylance, Ph.D. Dissertation, Univ. of Utah, 1968.
13. D. Roylance and K. L. DeVries, *Polym. Lett.*, **9,** 443, (1971).
14. R. P. Wool, *J. Polym. Sci.*, **13,** 1795, (1975).
15. V. I. Vettegren and I. I. Novak, *Sov. Physics-Solid State,* **15,** 957, (1973).
16. A. Peterlin, *J. Polym. Sci.*, **A-2,** 1151, (1969).
17. S. Nagou and K. Azuma, *J. Macromol. Sci.-Phys.*, **B16,** 435, (1979).
18. J. Park, Ph. D. Dissertation, Univ. of Utah, 1971.
19. D. W. van Krevelen, "Properties of Polymers," p. 77, Elsevier Publishing Co., (1972).
20. D. C. Prevorsek, Y. D. Kwon, and R. K. Sharma, *J. Mater. Sci.*, **12,** 2310, (1977).
21. R. Popli, Sc.D. Dissertation, Massachusetts Institute of Technology, 1980.